Available online at www.sciencedirect.com
ScienceDirect
Journal of Marine Systems 73 (2008) 76–86
JOURNAL OF MARINE SYSTEMS
www.elsevier.com/locate/jmarsys

Hydrography and biogeochemistry of the north western Bay of Bengal and the north eastern Arabian Sea during winter monsoon

K.K. Balachandran [a,*], C.M. Laluraj [b], R. Jyothibabu [a], N.V. Madhu [a], K.R. Muraleedharan [a], J.G. Vijay [a], P.A. Maheswaran [c], T.T.M. Ashraff [a], K.K.C. Nair [a], C.T. Achuthankutty [a]

[a] National Institute of Oceanography, Regional Centre, P.B. No.1913, Dr. Salim Ali Road, Cochin-682 018, India
[b] National Centre for Antarctic and Ocean Research, Headland Sada, Goa, India
[c] Naval Physical Oceanographic Laboratory, Trikkakara, Cochin-682 022, India

Received 29 August 2006; received in revised form 10 September 2007; accepted 12 September 2007
Available online 10 October 2007

Abstract

The north eastern Arabian Sea and the north western Bay of Bengal within the Indian exclusive economic zone were explored for their environmental characteristics during the winter monsoons of 2000 and 2001 respectively. The two regions were found to respond paradoxically to comparable intensities of the atmospheric forcing. There is an asymmetry in the net heat exchange of these two basins with atmosphere because of the varying thickness of barrier layer. During winter, the convective mixing in the Arabian Sea is driven by net heat loss from the ocean, whereas the Bay of Bengal does not contribute to such large heat loss to the atmosphere. It appears that the subduction of high saline Arabian Sea water mass is the mechanism behind the formation of a barrier layer in the northeast Arabian Sea; whereas that in the Bay of Bengal and the southeast Arabian Sea are already established as due to low saline water mass. The weak barrier layer in the Arabian Sea yields to the predominance of convective mixing to bring in nitrate-rich waters from the deeper layers to the surface, thereby supporting enhanced biological production. On the other hand, the river discharge into the Bay of Bengal during this period results in the formation of a thick and stable barrier layer, which insulates vertical mixing and provide oligotrophic condition in the Bay.

Keywords: Stratification; Barrier layer; Thermal inversion; North eastern Arabian Sea; North western Bay of Bengal; Winter cooling; Primary production

1. Introduction

The Northern Indian Ocean comprising of the Arabian Sea (AS) and the Bay of Bengal (BB) separated by the Indian peninsula, are tropical basins experiencing intense meteorological forcing, but differing widely in their upper ocean hydrology. The negative water balance associated with excess evaporation over precipitation and intrusion from Mediterranean Sea makes AS high saline (>36), whereas the excessive river run off into BB (1.625×10^{12} m^3y^{-1}, Subramanian, 1993) leads to a positive water balance (P-E=0.8 m y^{-1}, Ramanathan and Pisharody, 1972) and low salinity (<33). A dissimilarity that is observed in the winds over the two basins is that during the summer monsoon, winds are stronger in the AS than in the BB, whereas winds are of similar intensities during the winter

* Corresponding author. Tel.: +91 484 2390814; fax: +91 484 2390618.
E-mail address: kkbala@niokochi.org (K.K. Balachandran).

0924-7963/$ - see front matter © 2007 Elsevier B.V. All rights reserved.
doi:10.1016/j.jmarsys.2007.09.002

monsoon (Shenoi et al., 2002). It is well established that the AS is biologically more productive during summer monsoon, whereas the BB is traditionally considered to be a less productive system (Radhakrishna et al., 1978; Bauer et al., 1991; Brock et al., 1991; Prasannakumar et al., 2001a, 2002; Madhupratap et al., 2003). The north eastern Arabian Sea (NEAS) continues to sustain fairly high biological production during the winter monsoon also due to the nutrient entrainment into the euphotic layer by winter cooling-driven surface convection (Madhupratap et al., 1996; Prasannakumar et al., 2001a, 2001b). It is intriguing as to why in such a case, this 'biological niche' is elusive in the north western Bay of Bengal (NWBB), which also experiences a similar atmospheric forcing during winter. Although the extant of literature from the monsoon observations tends to emphasize its relation to heavy cloud cover, turbidity, low nutrient availability etc., the real mechanism that inhibits the carbon productions remains unresolved. An earlier report has attributed the difference in the biological production of these two basins during the winter monsoon to the strong thermohaline stratification in the BB (Jyothibabu et al., 2004). In this paper, we demonstrate that the significance of a thick barrier layer (BL) in the NWBB compared to a thin BL in the NEAS is the mechanism behind the contrasting biogeochemistry of the two basins during winter monsoon.

2. Sampling and analysis

The hydrographic data from the NEAS were collected during the winter monsoon of 2000 (FORV Sagar Sampada cruise no. 190 from 29th Nov–5th Jan.) and those from the NWBB (Fig. 1) were collected during the early winter monsoon of 2001 (FORV Sagar Sampada cruise no. 198 from 20th Nov–18th Dec.). The total number of stations sampled were 16 in the NEAS along 3 transects (Lat. 17°, 19° and 21° N, Long. 67–73° E) and 12 along 3 transects in the NWBB (Lat. 17°, 19° and 20.5° N, Long. 82–89° E). Surface meteorological parameters were taken at every 10 min using the ship based Automated Data Acquisition Software System. Vertical profiles of temperature (accuracy ± 0.001 °C) and salinity (accuracy ± 0.0001) were recorded at 1 m vertical intervals up to 1000 m. Seawater samples were collected from standard depths at all the stations using a Seabird CTD rosette system fitted with 12 Niskin bottles, each of 1.8 l capacity. CTD salinities were calibrated with on-deck analysis of discrete samples using a Guideline 8400 AUTOSAL (Ocean Scientific International, Pertersfield, UK). The samples were analyzed for nitrite, nitrate, phosphate and silicate with an onboard Auto Analyzer (Skalar Analytical, Breda, Netherlands) and dissolved oxygen for the corresponding depths following Winkler titration method (Grasshoff et al., 1983). Chlorophyll *a* and *in situ* primary productivity measurements were carried out from two stations in each transect representing coastal and oceanic regions respectively (Fig. 1). Primary production (PP) was measured by the radiocarbon (^{14}C) method (UNESCO, 1994; Bhattathiri et al., 1996). Water samples were taken from 7 depths (surface, 10, 20, 50, 75, 100 and 120 m) using Go-flo samplers and were transferred to 300 ml polycarbonate bottles (Nalgene, Germany). Each bottle was spiked with 1 ml of $NaH^{14}CO_3$ (5 μCi ml^{-1}, Board of Radioisotope Technology, Department of Atomic Energy, India) and the bottles were suspended at the approximate depths of sampling using a polypropylene line attached to a buoy. Three light bottles and one dark bottle were used at each depth. The incubation lasted from 1 h before sunrise to 30 min after sunset, after which the samples were retrieved and filtered through GF/F filters (pore size 0.7 μm) under gentle suction. The filters were exposed to concentrate HCl fumes to remove excess inorganic carbon and transferred to scintillation vials for subsequent estimation. A day before analysis, 5 ml of liquid scintillation cocktail (Sisco Research Laboratory, Mumbai) was added to the vials and the activity counted in a scintillation counter (Wallace 1409 DSA, Perkin-Elmer, USA). The disintegration per minute (DPM) was converted into daily production rates (mgC m^{-2} d^{-1}) taking into account the initial activity in the bottles and the initial adsorption of ^{14}C by particles in the bottles (Strickland and Parsons, 1972). Samples for chlorophyll (Chl a) analysis were also taken from the same casts as that of primary productivity (Fig. 1). One litre of water sample from each depth was filtered through GF/F filters (pore size 0.7 μm). Chl a estimation was carried out using a spectrophotometer (Perkin Elmer, USA), after extracting with 10 ml 90% acetone in the dark (Strickland and Parsons, 1972). Column PP (mgCm^{-2} d^{-1}) and column Chl a (mg m^{-2}) were calculated by integrating over 120 m depth. In the present study, since the driving force behind blooming of phytoplankton in surface waters is the availability of nutrients (especially nitrogen) and its entrainment into the euphotic zone, we examine the upper 200 m water column to understand the processes that regulate the supply of nitrogen into the surface layers of these two basins.

The mixed layer depth (MLD) discussed here is defined as the depth at which the density of the seawater changes ("$\Delta\sigma_\theta$") by 0.2 from the surface value (Sprintall and Tomczak, 1993). Note that even though this way of calculation of MLD may not hold good for the two basins, a comparison can be made only when physical properties are normalized to one format. The ILD, the

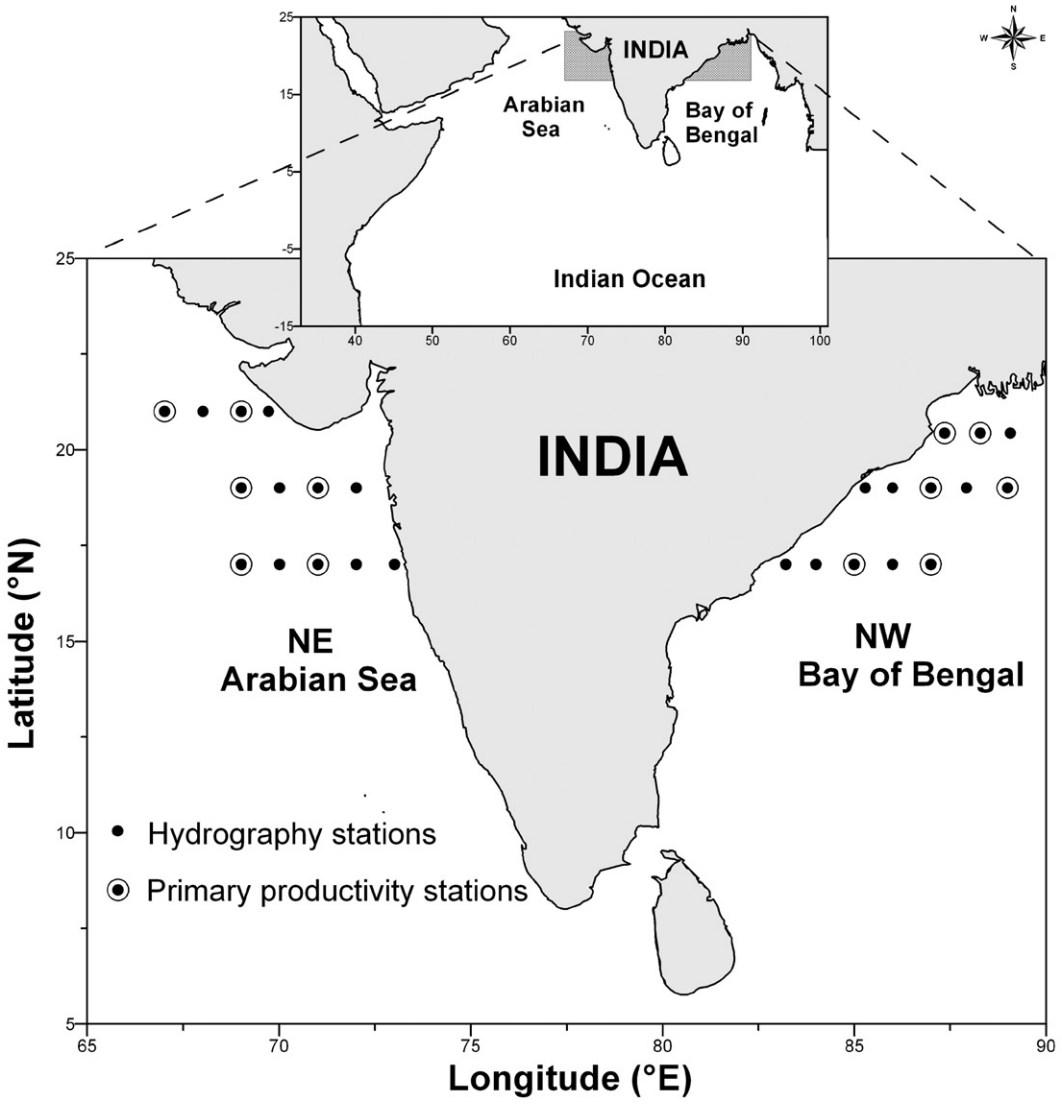

Fig. 1. Study region showing the station locations in the northeastern Arabian Sea and north western Bay of Bengal.

depth of the top of the thermocline, is defined as the depth at which surface temperature decreases by 1 °C from sea surface temperature (Kara et. al., 2000; Rao and Sivakumar, 2003). The above definition of ILD holds good only for normal temperature distribution. Therefore, for profiles with temperature inversion, ILD is defined as the depth at which the temperature at the base of the inversion layer is equal to the temperature at the top of the inversion layer. This definition is valid as the inversion layer is embedded within the barrier layer and it is sustained by the haline stratification (Pankajakshan et al., 2002, 2007a). The barrier layer (BL) in the present study is computed as the difference between ILD and MLD following the method of Lukas and Lindstrom (1991). The stability of water column represented by Brunt–Väisälä frequency (N) was computed following adiabatic leveling method (Bray and Fofonoff, 1981).

3. Results

3.1. General hydrography

The NEAS and the NWBB exhibited more or less uniform variations in the meteorology at comparable latitudes. Generally, the air temperature (AT) decreased from 30.5° to 24.5 °C along lat. 17°–21° N in the NEAS and from 29.4° to 25.5 °C along lat .17°–20.5° N in the NWBB, whereas the atmospheric pressure ranged

marginally between 1010 and 1015 mb (Jyothibabu et al., 2004). Both regions experienced moderate winds (6–9 m/s), except in the region between 19° and 20.5° N in the NWBB, where the wind was comparatively weak (~4 m/s). The sea surface temperature (SST) varied from 25.9–27.4 °C in the NEAS and from 26.1–27.8 °C in the NWBB, the cooler water being observed towards north.

3.2. Northeastern Arabian Sea

The excess evaporation over precipitation and the presence of several high density waters (Red Sea Water and Persian Gulf Water) provide AS a unique property of sustaining high saline water mass. During winter season, the evaporative cooling results in the formation of dense water mass (Arabian Sea High Salinity Water Mass), which on sinking deepens the mixed layer (ML). The heat loss by evaporation and sinking of the surface waters initiates convective mixing (Madhupratap et al., 1996). During the present study, the ML in the NEAS along lat. 17, 19 and 21° N of the NEAS was deep, but the BL, observed at some locations (maximum 35 m), though weak, is quite interesting (Fig. 2).

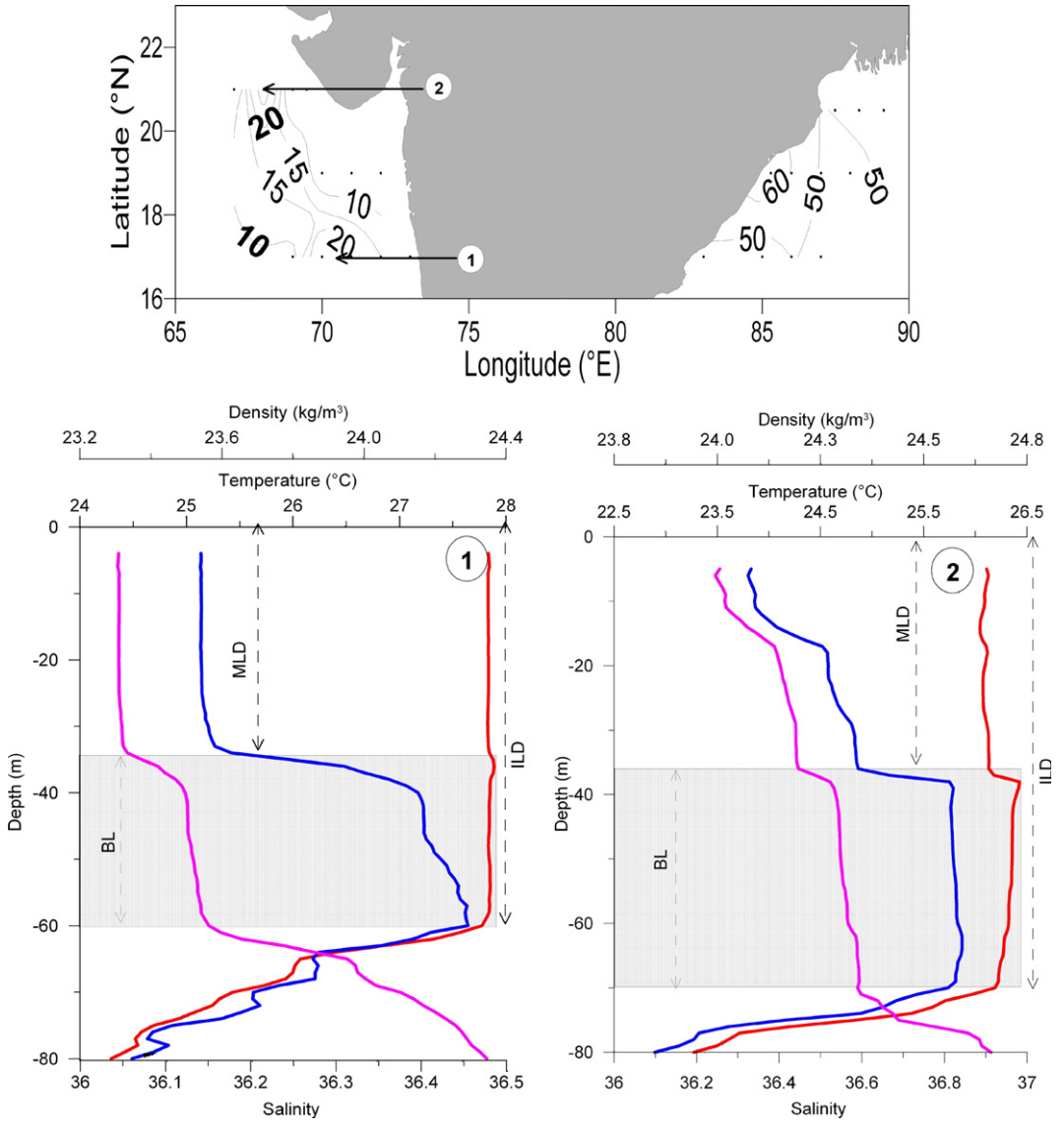

Fig. 2. Top panel — Horizontal distribution of barrier layer depth in meters in the NEAS (Dec.2000) and NWBB (November 2001). Bottom panel — Thermohaline stratification at two different locations (shown in the top panel) of the NEAS at (1) 17° N 70° E and (2) 21° N 68° E.

3.2.1. Barrier layer in the NEAS

The formation of BL in the BB and SEAS is well known (Gopalakrishna et al., 2005; Shenoi et al., 2005; Durand et al., 2007; Pankajakshan et al., 2007), but very little information is available for the occurrence of the same in the NEAS. Presence of a thick BL (20–50 m) in the NEAS is reported during January–February (Pankajakshan et al., in press). In the present study (December), we have identified a BL of more than 25 m thick at two locations (Fig. 2, top panel). The vertical profiles of the thermohaline properties at 17° N 70° E and 21° N 68° E (Fig. 2, bottom panel) indicate a shallower isohaline layer than isothermal layer. It should be mentioned here that, these locations were characterized by a thin layer containing a well developed salinity maximum (>36.2) at its base, located above the top of the thermocline and a deeper layer of lower salinity. This saline layer originates at the surface in the north AS partially in response to high evaporation, and subsequently gets subducted to 50–60 m while moving towards the NE boundary, which is known as the Arabian Sea High Salinity Water Mass (Kumar and Prasad, 1999; Pankajakshan et al., in press). It is evident that the subduction of this ASHSW along the isopycnals has initiated the BL in the NEAS (Fig. 2, lower panel). The significance of this observation is that, BL formation due to subducted high salinity waters has been so far reported only from the northwest equatorial Atlantic (Sprintall and Tomczak, 1993). A comparison of the BL from the present study in the NWBB and the NEAS with that of Pankajakshan et al. (2007a, in press) also supports a deep BL in the former and a shallow BL in the latter. Thus, the BL formation in the NEAS is due to the high salinity water mass; whereas that in the BB and SEAS is due to low saline water mass.

As a result of the thin BL and a thick ML, the convective mixing became predominant and brought the 2 μM NO_3 from the top of the thermocline at 17° N which eventually spread out along the entire surface waters of 19 and 22° N (Fig. 3). The region north of 17° N was uniformly enriched in nitrate and phosphate (0.4 μM) right up to the surface (Fig. 4) and along the

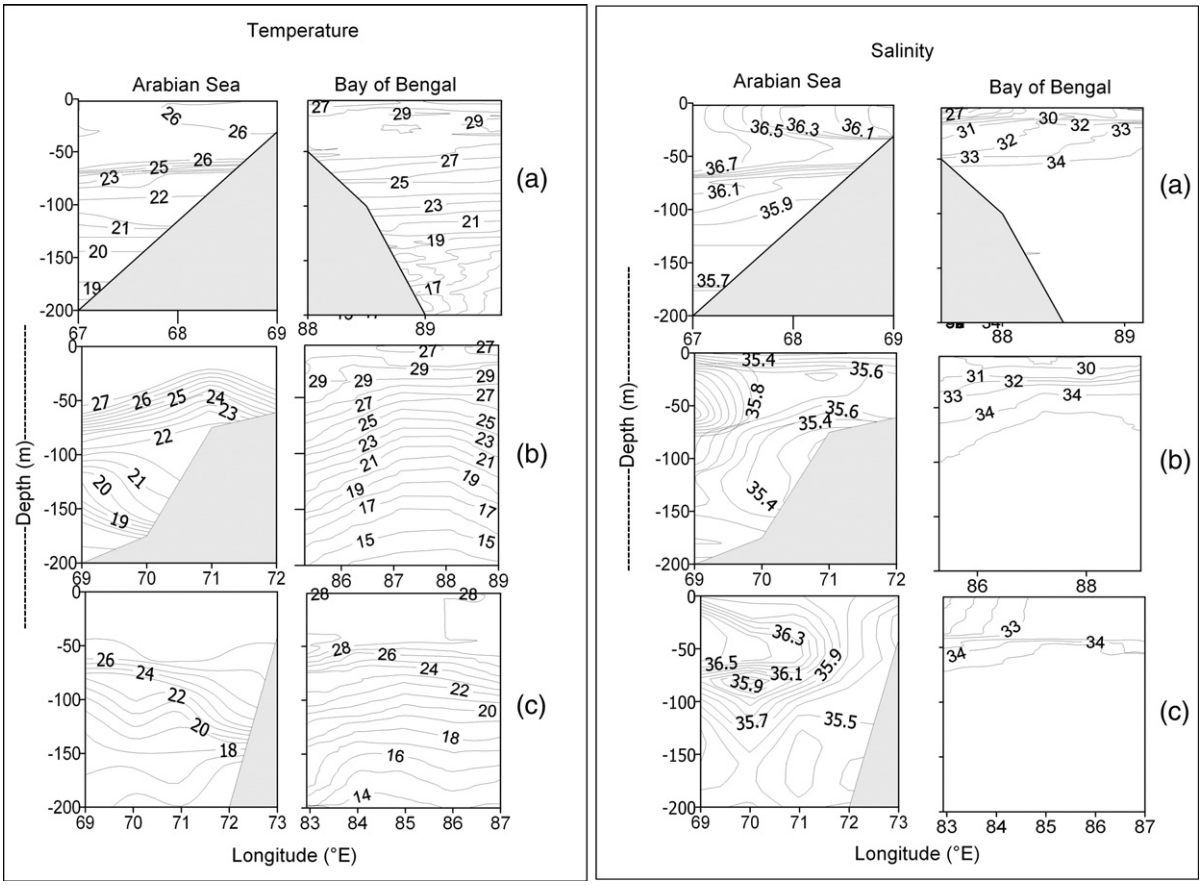

Fig. 3. Vertical sections of temperature (°C) in the left and salinity in the right panel along 17° N (a), 19° N (b) and 21° N (c) in the NEAS and 17° (a), 19° (b) and 20.5° N (c) in the NWBB.

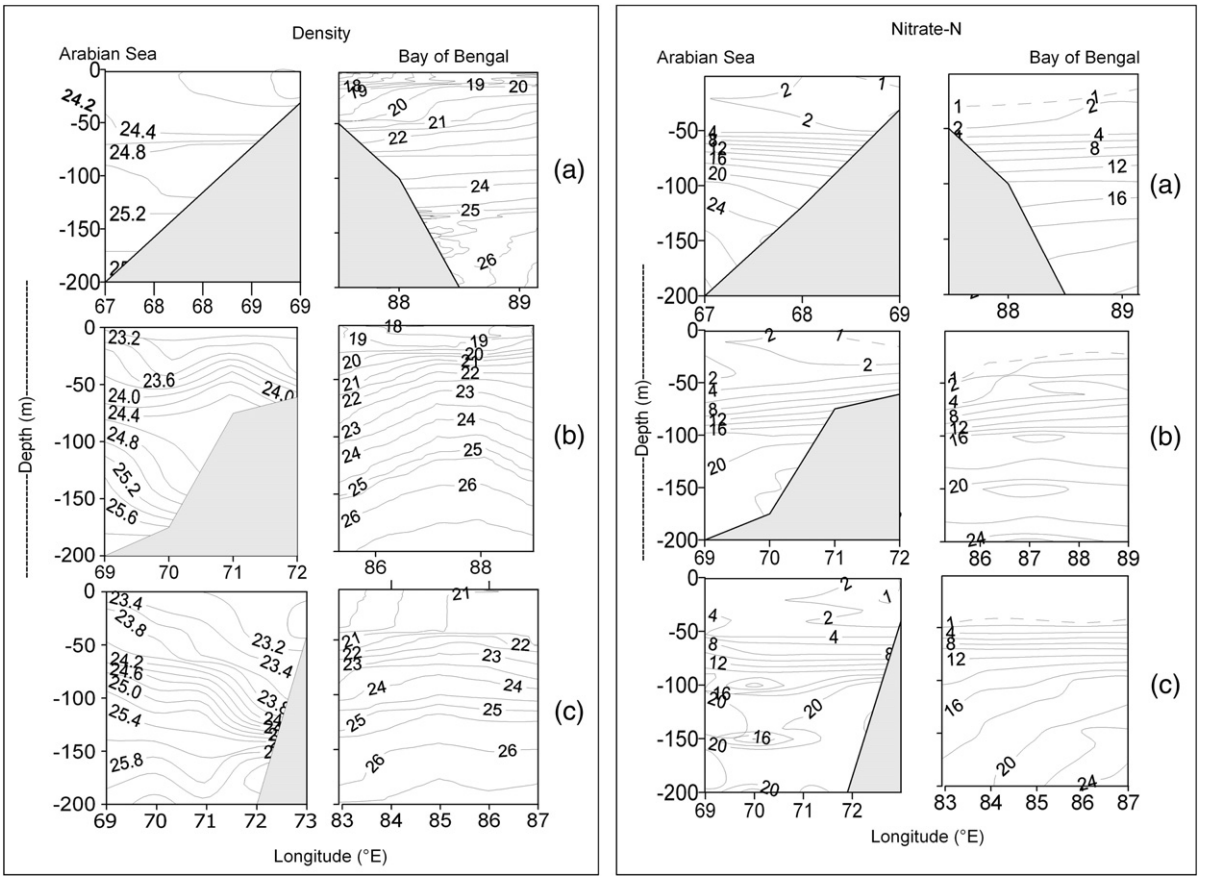

Fig. 4. Vertical sections of density (kg/m^3) in the left and nitrate (μM) in the right panel along 17° N (a), 19° N (b) and 21° N (c) in the NEAS and 17° N (a), 19° N (b) and 20.5° N (c) in the NWBB.

coast up to 72° E (17° N).It was spreading out further offshore along 21° N and 68° E, whereas silicate (1 μM) did not show any repletion (Fig. 5) The impoverishment of the surface waters with nutrients at locations where the BL thickness was >25 m is noticeable.

3.3. Northwestern Bay of Bengal

It can be seen from the vertical sections of temperature and density of the northern bay that instead of a well-defined thermocline, the subsurface layers (30–50 m) were increasingly getting warmer (>3 °C) towards the northern latitudes (Fig. 3). As the fresh water discharge spreads over the sea surface, the winter cooling further modifies to trap the warm BB waters just below a thin lid (<30 m) of cool surface waters The distribution of salinity in the NWBB indicates the influence of fresh water run off from the land. The low salinity (~25) observed towards the coasts between 17 and 20.5° N may be due to the fresh water discharges from Godavari, Mahanadi and Ganges rivers. This fresh water flow imposes stratification with a salinity gradient of 1.8 in the upper 30 m at 17° N (31.6–33.4), increasing to 5.5 (26.5–31) at 20.5° N (Fig. 3). Salinity increased gradually from 30 to 75 m, and below this depth, it remained homogeneous.

The subsurface layer was also impoverished in nutrients, as the 1 μM nitracline was suppressed to below MLD (30–50 m) along all the latitudes (Fig. 4). Dissolved inorganic phosphate was also low (DIP<0.2 μM), but silicate was fairly distributed (>2 μM) in surface and increased towards the northern latitudes (20.5° N), indicating its river source (Fig. 5). The salinity gradient was found to intensify towards west in all transects, due to the increased fresh water discharge. It is evident from Fig. 6 that in the NWBB, the 20–60 m thick subsurface layer has more stability (120 cycles/h). It is therefore assumed that the fresh water flow stabilizes the euphotic zone by forming a deep BL with a shallow ML embedded in it, which insulates the entrainment of nutrient-rich deep waters into the mixed layer.

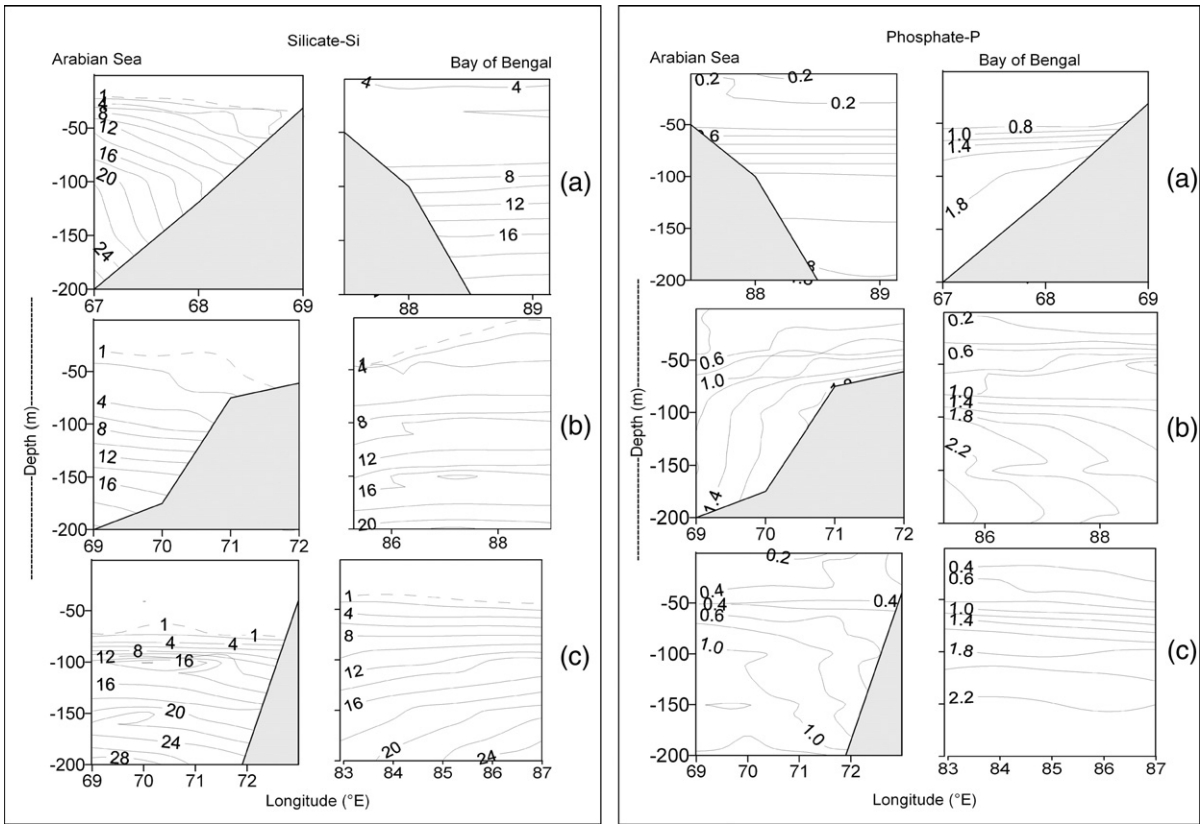

Fig. 5. Vertical sections of silicate (μM) in the left and phosphate (μM) in the right panel along 17° N (a), 19° N (b) and 21° N (c) in the NEAS and 17° (a), 19° (b) and 20.5° N (c) in the NWBB.

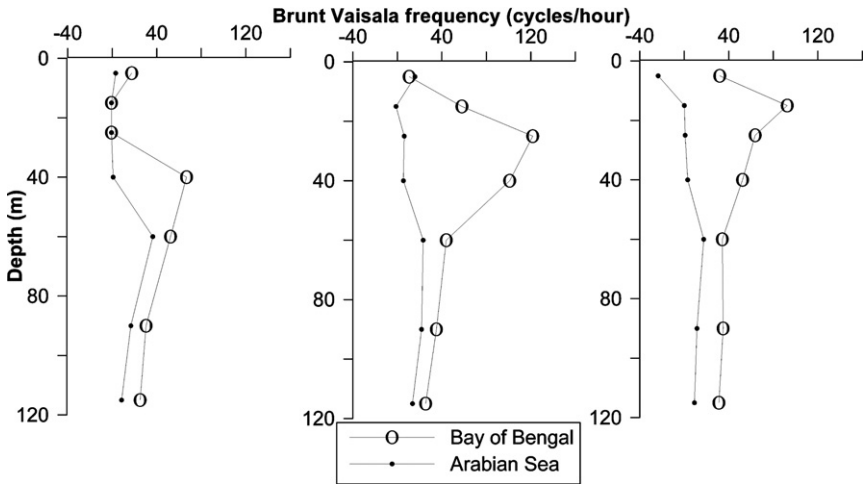

Fig. 6. Vertical profiles of Brunt–Vaisala stability frequency (cycles per hour) along 17° N (a), 19° N (b) and 21° N (20.5° for NWBB). Solid circle represents the AS and open circle represents the BB.

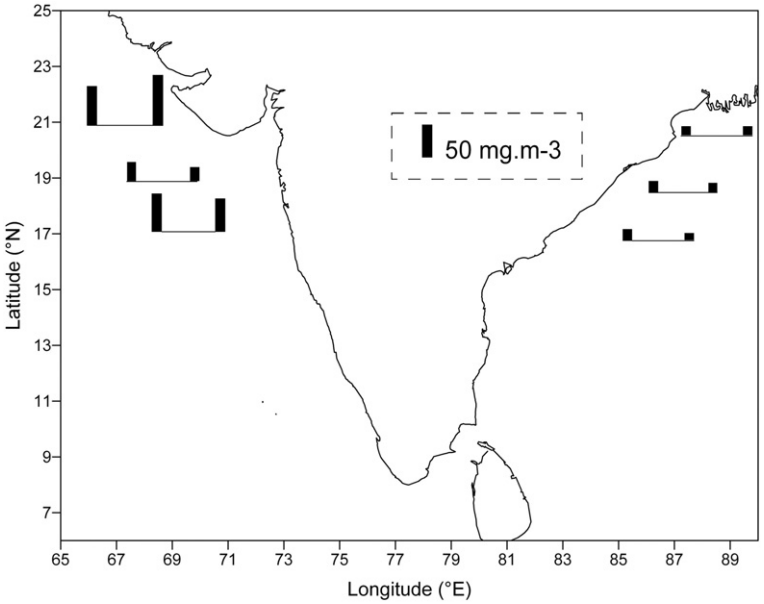

Fig. 7. Integrated column chlorophyll a (mg m^{-3}) during Dec. 2000 (in NEAS) and Nov.–Dec. 2001 (in NWBB).

3.4. Winter cooling and environmental responses — a comparison

It is interesting to note that while the intensities of atmospheric forcing were almost similar in both regions, the NEAS showed enhanced biological activity, whereas the NWBB remained low in the primary production. This suggests that, whereas the NEAS is vulnerable to atmospheric forcing, the NWBB remains stable due to the formation of a thick BL. In the NEAS, the convective mixing is strong enough to erode the BL and bring the nutrient-rich waters into the ML. This is a preconditioning for biological production evidenced by an increased column chlorophyll *a* biomass along 17°, 19° and 21° N (45–58 mg m^{-3}, 19–25 mg m^{-3} and 82–56 mg m^{-3}) respectively (Fig. 7). The corresponding

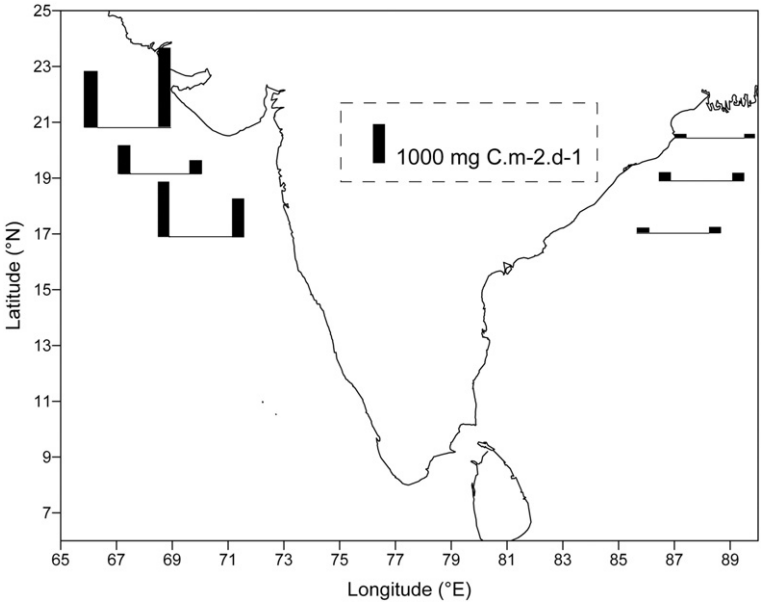

Fig. 8. Integrated column primary productivity (mgC m^{-2} d^{-1}) during Dec. 2000 (in NEAS) and Nov.–Dec. 2001 (in NWBB).

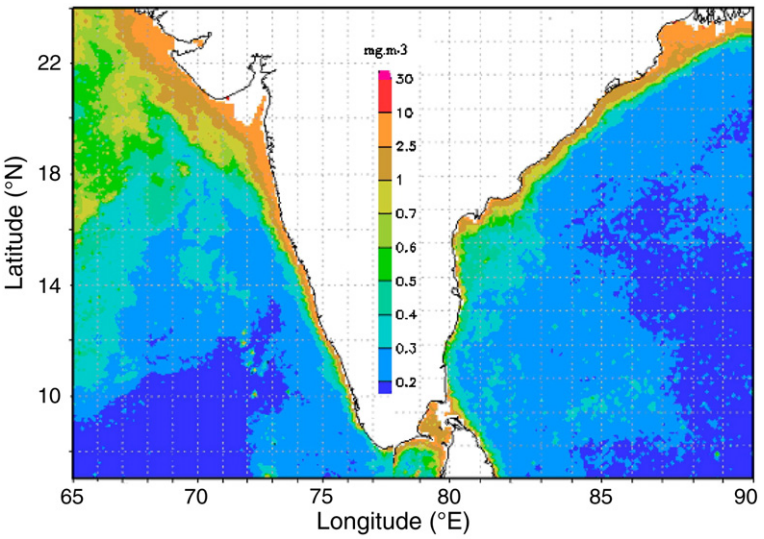

Fig. 9. Surface chlorophyll *a* distribution (monthly average compiled from Sea WiFS) in the AS (Dec. 2000) and the BB (Nov–Dec 2001).

primary production (PP) ranged from 1016–1348 $mgCm^{-2}d^{-1}$, 373–731 $mgCm^{-2}d^{-1}$ and 1363–1854 $mgCm^{-2}d^{-1}$, respectively (Fig. 8). In contrast, the thick BL in the NWBB prevented the nitrogen entrainment from deeper waters. Hence, the biological activity was kept low along 17, 19 and 20.5° N (column chlorophyll *a* 14–9, 15–13 and 9–9 mg m^{-3}, respectively). The PP along these latitudes (Fig. 8) also remained low (101–145, 164–187 and 87–115 $mgCm^{-2}d^{-1}$, respectively). Surface chlorophyll *a* derived from satellite imageries (SeaWiFS, Fig. 9) during the respective periods also indicated an increase in the biomass in the NEAS compared to NWBB, corroborating our studies. It is estimated that the average column chlorophyll biomass sustained in the NEAS was 10 times higher than that in the NWBB (Table 1).

Table 1
Average values of column chlorophyll *a* (mg m^{-3}) and column primary production (mgC m^{-2} d^{-1}) in the coastal and oceanic stations of NEAS and NWBB

Latitude ° N	NEAS coastal	NEAS oceanic	NWBB coastal	NWBB oceanic
Chlorophyll a (mg m^{-3})				
17	45	58	14	9
19	19	25	15	13
20.5	–	–	9	9
21	82	56	–	–
Primary production (mgC m^{-2} d^{-1})				
17	1016	1348	145	101
19	373	731	187	164
20.5	–	–	115	87
21	1854	1363	–	–

4. Discussion

The mixed-layer dynamics have a strong influence on both water mass formation and hence, nutrient availability in the surface layers, which modulate biological productivity. The formation and spreading of BL has a significant role in maintaining the warm SST (>28 °C) in the NWBB. During winter monsoon, the northern bay experiences strong temperature inversions (up to 3 °C) in the subsurface layer, following which, a thick BL (~50 m) is spatially organized along the entire area. Since the inversion layer is embedded within the BL and exhibits large salinity stratification, the BL in the bay is a more stable and sustained feature (Pankajakshan et al., 2002). The thick BL acts as a barrier for the transfer of momentum, heat and nutrients, as observed in the present study. During winter monsoon, the ML in the NEAS is deeper (60–70 m) and cooler than that of the NWBB (8–30 m). The main reason for this difference is the asymmetry in the net heat exchanged between the ocean and atmosphere of these two basins (Prasad, 2004). The latent heat flux is dependant on humidity; the drier air over the AS facilitates enhanced cooling. The evaporative cooling leads to buoyancy of the surface waters owing to net heat loss from the ocean. The buoyancy flux due to salt has an influence on the deepening of ML (>80 m) in the AS, but is limited to shallow depths (8–30 m) in the BB (Prasad, 1997; Prasad, 2004). Thus, a comparatively

weaker winter cooling (loss of net heat flux) in the NWBB had resulted in less nutrient supply to the surface leading to low biological production. However, cyclonic storms are found to disrupt the BL bringing nutrient-rich waters from the deep to enhance phytoplankton production in the BB (Rao et al., 1994; Madhu et al., 2000).

The situation is different in the AS, as there is no fresh water input during the period and the BL is very weak over the entire northeast AS (Fig. 2). This is further evidenced by the low stability of the NEAS surface waters compared to the NWBB (Fig. 6). The maximum stability of the upper 120 m water column in the NWBB was 70–120 cycles/h (between 17 and 21° N) during winter, while that in the NEAS for corresponding latitudes was <20 cycles/h.

It is evident that the enrichment of the euphotic layer with silica was not favoring primary production in the NWBB, because according to the Redfield ratio, the available phosphorus should have a minimum nitrate (>1 μM) to support phytoplankton production (Redfield et al., 1963). In contrast, the NEAS was uniformly enriched in nitrate and phosphate (0.4 μM) in the euphotic zone from 17° to 21° N, whereas the silicate (1 μM) remained comparatively low (Figs. 4 and 5). The rising of the nitracline triggered enhanced biological activity in the region because, there was a net increase in the ratio of *N*: Si to ~2/1, vs. ~1 assumed to be the approximate ratio of uptake by diatoms (Morrison et al., 1998). Thus, there appears to be silica limiting for the diatom growth in the NEAS, as observed in the open ocean upwelling regions. This is an anomaly since it has been observed that Si concentrations of the AS are higher than minimum *N* concentration in surface waters and a net removal of Si may not be possible below 0.6–0.8 μM in warm waters (David et al., 1994; Brezinski and Nelson, 1995). Because of the insignificant contribution of fresh water flow into the AS during winter monsoon, it is possible that silica may be more limiting to diatom blooms in the continental shelf than nitrogen, a situation that has been described only for open-ocean upwelling regions (Dugdale et al., 1995; Dugdale and Wilkerson, 1998).

5. Summary and conclusions

The observations show that during the winter monsoon, the atmospheric forcing and continental drainage influence the biogeochemistry of the NEAS and the NWBB, respectively. Although the winter evolutions of oceanographic features resulted in convective mixing and enhanced biological production in the NEAS, the same intensity of winter cooling resulted in low biological production in the NWBB. This is primarily due to the increased stability of the water column in the NWBB, by the formation of a thick BL having an inversion layer embedded in it, which restricted the entrainment of nutrients from subsurface waters. It should be noted that an increased nitrogen loading (4.5 mg $Nm^{-2}d^{-1}$) by freshwater did not contribute repletion of nitrate concentration in the surface waters of the BB, and the resultant low biological activity inferred from the low pCO_2 concentrations in this region (Kumar et al., 1996). In conclusion, this study shows that the biological activity in the northern Indian Ocean is controlled by Air↔Sea↔Land interactions on varying geographic scale. The Air–Sea interactions in the NWBB are insignificant, where the hydrography is mainly controlled by Land–Sea interactions. In contrast, the negative water balance and the Arabian Sea High Salinity Waters make the NEAS highly vibrant to Air–Sea interactions, where atmospheric forcing dictates the upper ocean hydrography. This communication shows that high saline waters are the principal cause of the formation of BL in the NEAS, whereas those in the BB and SEAS are due to low saline water mass.

Acknowledgements

We thank Dr. S.R. Shetye, Director, National Institute of Oceanography, Goa and Dr. N. Bahulayan, Scientist-in-Charge, Regional Centre, Cochin for the encouragement. We are grateful to all the participants of cruise no. 190 and 198 of FORV Sagar Sampada for the help. This investigation was carried out under the Marine Research-Living Resource programme funded by Centre for Marine Living Resources and Ecology (CMLRE), Ministry of Earth Sciences, New Delhi. The constructive comments given by the two anonymous reviewers have helped us to improve the manuscript substantially. We are grateful to Prof. Wolfgang Fennel for his critical suggestions and useful editing. This is NIO Contribution 4295.

References

Bauer, S., Hitchcock, G.L., Olson, D.B., 1991. Influence of monsoonally-forced Ekman dynamics upon the surface-layer depth and plankton biomass, distribution in the Arabian Sea. Deep-Sea Res. 38, 531–553.

Bray, N.A., Fofonoff, N.P., 1981. Available potential energy for MODE eddies. J. Phys. Oceanogr. 11, 30–46.

Bhattathiri, P.M.A., Pant, A., Sawant, S., Gauns, M., Matondkar, S.G.P., Mohanraju, R., 1996. Phytoplankton production and

chlorophyll distribution in the eastern and central Arabian Sea in 1994-1995. Curr. Sci. 71, 857–862.
Brezinski, M.A., Nelson, D.M., 1995. The annual cycle in the Sargasso Sea near Bermuda. Deep-Sea Res. 42, 1215–1237.
Brock, J.C., Mc Clain, C.R., Luther, M.E., Hay, W.W., 1991. The phytoplankton bloom in the northwestern Arabian Sea during the southwest monsoon of 1979. J. Geophys. Res. 96, 733–750.
David, K., Young, John, Kindle, C., 1994. Physical processes affecting availability of dissolved silicate for diatom production in the Arabian Sea. J.Geophys. Res. 99, 22619–22632.
Dugdale, R.C., Wilkerson, F.P., Mineas, H.J., 1995. The role of a silicate pump in driving new production. Deep-Sea Res. 42, 697–719.
Dugdale, R.C., Wilkerson, F.P., 1998. Silicate regulation of new production in the equatorial Pacific upwelling. Nature 391, 270–273.
Durand, F., Shankar, D., De Boyer, Montegut, Shenoi, S.S.C., Blanke, B., Madec, G., 2007. Modeling the barrier layer formation in the southeastern Arabian Sea. Am. Meteor. Soc. 20, 2109–2120. doi:10.1175/JCL14112.1.
Gopalakrishna, V.V., Johnson, Z., Salgaonkar, G., Nisha, K., Rajan, C.K., Rao, R.R., 2005. Observed variability of sea surface salinity and thermal inversion in the Lakshadweep Sea during contrast monsoons. Geophys. Res. Let. 32, L18605. doi:10.1029/2005GL023280.
Grasshoff, K., Ehrhardt, M., Kremling, K., 1983. Method of seawater analysis. Verlag Chemie, Weinheim, p. 419.
Jyothibabu, R., Maheswaran, P.A., Madhu, N.V., Mohammed, A.T.T., Vijay, J.G., Haridas, P.C., Venugopal, P., Revichandran, C., Nair, K.K.C., Gopalakrishnan, T.C., 2004. Differential response of winter cooling on biological production in the northeastern Arabian Sea and northwestern Bay of Bengal. Curr. Sci. 87, 783–791.
Kara, A.B., Rochford, P.A., Hurlburt, H.E., 2000. An optimal definition for ocean mixed layer depth. J. Geophys. Res. 105, 16,803–16,821.
Kumar, D.M., Naqvi, S.W.A., George, M.D., Jayakumar, D.A., 1996. A sink for atmospheric CO_2 in the NIO. J. Geophys. Res. 101, 18121–18125.
Kumar, P.S., Prasad, T.G., 1999. Formation and spreading of Arabian Sea high salinity water mass. Journal of Geophysical Research 104, 1455–1464.
Lukas, R., Lindstrom, E., 1991. The mixed layer of the western equatorial Pacific Ocean. J.Geophys. Res. 96, 3343–3357.
Madhu, N.V., Maheswaran, P.A., Jyothibabu, R., Sunil, V., Revichandran, C., Balasubramanian, T., Gopalakrishnan, T.C., Nair, K.K.C., 2000. Enhanced biological production off Chennai triggered by October super cyclone (Orissa). Curr. Sci. 82, 1472–1479.
Madhupratap, M., Kumar, S.P., Bhattathiri, P.M.A., Kumar, M.D., Raghukumar, S., Nair, K.K.C., Ramaiah, N., 1996. Mechanism of the biological response to winter cooling in the northern Arabian Sea. Nature 384, 549–552.
Madhupratap, M., Mangesh, G., Ramaiah, N., Prasannakumar, S., Muraleedharan, P.M., de Sousa, S.N., Sardesai Usha, M., 2003. Biogeochemistry of the Bay of Bengal during summer monsoon 2001. Deep-Sea Res. II 50, 881–886.
Morrison, J.M., Codispoti, L.A., Gaurin, S., Jones, B., Manghnani, V., Zheng, Z., 1998. Seasonal variation of hydrographic and nutrient fields during the US JGOFS Arabian Sea Process Study. Deep Sea Res. II 45, 2053–2101.
Pankajakshan, T., Gopalakrishna, V.V., Muraleedharan, P.M., Reddy, G.G., Nilesh, A., Srikant, S., 2002. Surface layer temperature inversion in the Bay of Bengal. Deep-Sea Res. II 49, 1801–1818.
Pankajakshan, T., Muraleedharan, P.M., Rao, R.R., Somayajulu, Y.K., Reddy, G.V., Revichandran, C., 2007. Observed seasonal variability of barrier layer in the Bay of Bengal. J. Geophys. Res. 112. doi:10.1029/2006JC003651.
Pankajakshan, T., Prasad, T., Raghu, M., Muraleedharan, P.M., Rao, R.R., Somayajulu, Y.K., Gopalakrishna, V.V., Reddy, G.V., Revichandran, C., in press. Seasonal variability of observed and modeled barrier layer thickness in the Arabian Sea. J. Phys. Oceanogr.
Prasad, T.G., 1997. Annual and seasonal mean buoyancy fluxes for the tropical Indian Ocean. Curr. Sci. 73, 667–674.
Prasad, T.G., 2004. A comparison of mixed-layer dynamics between the Arabian Sea and Bay of Bengal: One-dimensional model results. J. Geophys. Res. 109, C03035. doi:10.1029/2003JC002000.
Prasannakumar, S., Madhupratap, M., Dileepkumar, M., Muraleedharan, P.M., de Souza, S.N., Gauns, M., Sarma, V.V.S.S., 2001a. High biological productivity in the central Arabian Sea during summer monsoon driven by Ekman pumping and lateral advection. Curr. Sci. 81, 1633–1638.
Prasannakumar, S., Ramaiah, N., Gauns, M., Sarma, V.V.S.S., Muraleedharan, P.M., Raghukumar, S., Dileepkumar, M., Madhupratap, M., 2001b. Physical forcing of biological productivity in the northern Arabian Sea during the northeast monsoon. Deep-Sea Res. II 48, 1115–1126.
Prasannakumar, S., Muraleedharan, P.M., Prasad, T.G., Gauns, M., Ramaiah, N., de Souza, S.N., Sardesai, S., Madhupratap, M., 2002. Why is the Bay of Bengal less productive during summer monsoon compared to the Arabian Sea? Geophys. Res. Letters 29 (24), 2235. doi:10.1029/2002GL016013.
Radhakrishna, K., Bhattathiri, P.M.A., Devassy, V.P., 1978. Primary productivity of Bay of Bengal during August-September 1976. Indian J. Mar. Sci., 7, 94–98.
Ramanathan, K.R., Pisharody, P.R., 1972. Water balance — Indian Ocean in World Water Balance. Institute of Hydrologic Science. Genthbrugge, Belgium, pp. 39–41.
Rao, C.K., Naqvi, S.W.A., Kumar, M.D., Varaprasad, S.J.D., Jayakumar, D.A., George, M.D., Singbhal, S.Y.S., 1994. Hydrochemistry of Bay of Bengal: possible reasons for a different water-column cycling of carbon and nitrogen from the Arabian Sea. Mar. Chem. 47, 279–290.
Rao, R.R., Sivakumar, R., 2003. Seasonal variability of near-surface salinity and salt budget of the mixed layer of the north Indian Ocean. J.Geophys. Res. 108, 309. doi:10.1029/2001JC000907.
Redfield, A.C., Ketchum, B.H., Richards, A., 1963. The influence of organisms on the composition of seawater. In: Hill, M.N. (Ed.), The Sea, 2. Interscience, New York, pp. 26–77.
Shenoi, S.S.C., Shankar, D., Shetye, S.R., 2002. Differences in heat budgets of the near-surface Arabian Sea and Bay of Bengal: implications for the summer monsoon. J. Geophys. Res. 107 (C6), 5.1–5.14.
Shenoi, S.S.C., Shankar, D., Gopalakrishna, V.V., Durand, F., 2005. Role of ocean in the genesis and annihilation of the core of the warm pool in the southeastern Arabian Sea. Mausam 56, 147–160.
Sprintall, S.R., Tomczak, M., 1993. Evidence of the barrier layer in the surface layer of the tropics. Journal of Geophysical Research 97, 7305–7316.
Strickland, J.D.H., Parsons, T.R., 1972. A Practical Handbook of Sea Water Analysis (2nd Ed.). Bull. Fish. Res. Board Canada, p. 310.
Subramanian, V., 1993. Sediment load of Indian Rivers. Curr. Sci. 64, 98–930.
UNESCO, 1994. Protocols for the Joint Global Ocean Flux Study. Manuals and Guides, p. 190 (29).